SPLENOMEGALY AND MODIFIED ERYTHROPOIESIS IN KLF13$^{-/-}$ MICE

Adele R Gordon*[1], Susan V Outram*[2], Mohammad Keramatipour*[1], Catherine A Goddard[1], William H Colledge[3], James C. Metcalfe[1], Ariadne L. Hager-Theodorides[2], Tessa Crompton[2] and Paul R. Kemp[4]

[1]Section of Cardiovascular Biology, Department of Biochemistry, University of Cambridge, Downing Site, Cambridge, CB2 1QW [2]Division of Cell and Molecular Biology Sir Alexander Flemming Building Imperial College, South Kensington Campus, London, [3]Physiology, Development and Neuroscience, University of Cambridge, Downing Site, Cambridge or [4]National Heart and Lung Institute, Sir Alexander Flemming Building Imperial College, South Kensington Campus, London, SW7 2AZ

Running title: Erythropoiesis in *Klf13*$^{-/-}$ mice

***** These authors contributed equally to the work.

Address Correspondence to: Dr Paul Kemp, National Heart and Lung Institute, Imperial College, South Kensington Campus, London SW7 2AZ. Tel:+44 20 7594 1716. Fax +44 20 7594 3100. E.mail p.kemp@imperial.ac.uk,

To study the function of the Krüppel-like transcription factor KLF13 *in vivo* we generated mice with a disrupted *Klf13* allele. Whilst *Klf13*$^{-/-}$ mice are viable, fewer mice were present at 3 weeks than predicted by Mendelian inheritance. Viable *Klf13*$^{-/-}$ mice had reduced numbers of circulating erythrocytes and a larger spleen. The spleen contained an increased number of Ter119^{med}CD71^{hi}, Ter119^{hi}CD71^{hi} and Ter119^{hi}CD71^{med} cells but not Ter119^{hi}CD71^{-} cells indicating an increase in less mature erythroblasts. A higher proportion of the Ter119^{med}CD71^{hi} cells were proliferating indicating that the mice were under a degree of erythropoietic stress. These data indicate that KLF13 is involved in the normal control of erythropoiesis.

Erythrocytes differentiate from multi-potential haematopoietic stem cells through a series of intermediates. The first committed erythrocyte precursors are the burst forming unit cells (BFU-E) which differentiate into colony forming units (CFU-E) and then to proerythroblasts (1). As these cells differentiate further through the basophilic, polychromatic and orthochromatic erythroblast stages the nucleus shrinks and is finally shed as the cells become reticulocytes before becoming erythrocytes (2). During these later stages of differentiation the cells lose expression of CD71 and gain the expression of ter119 so that these cell surface markers can be used to differentiate the different cell stages (3). The process of erythrocyte differentiation is controlled by a number of different transcription factors and regulated such that under normal conditions sufficient erythrocytes are produced predominantly by the bone marrow but under conditions of erythropoietic stress (e.g. hypoxia) the number of erythrocytes can be increased and this occurs predominantly in the spleen (4,5).

Analysis of the transcriptional program controlling erythroblast differentiation has identified a number of different transcription factors that are critical to the normal development of erythrocytes (1,2,6). The best studied of these factors regulating erythroid differentiation is GATA-1 a zinc finger transcription factor initially identified as a protein that bound to the globin genes and activated their expression (7). Loss of GATA-1 leads to a failure of erythropoiesis early in gestation resulting in death of the embryos from severe anaemia by E10.5 (8). The erythroblasts in these embryos fail to develop past a pro-erythroblast like stage.

Another transcription factor that has been studied extensively in erythrocytes is the Krüppel-like factor (KLF) EKLF/KLF1, a member of a family of at least 16 transcription factors (9,10). Members of this family can both activate and repress transcription through interaction with a range of different transcription factors (e.g. the GATA factors and NF-κB) and co-factors (e.g. p300, mSin3A) (11-14). KLF1 was first identified as a CACC box binding factor expressed in erythroleukaemia cells but not in monocytes/macrophages (15). Mice that lack expression of *Klf1* die at E16 from a severe anaemia indicating a critical role for KLF1 in the formation of erythrocytes (16). At least 8 other xKLF proteins (KLF2- 5, 8 and 11- 13) are expressed in erythroid cell lines. Of these KLF2, 5, 8 and 13 have been shown to bind to CACCC boxes in globin promoters and can modify promoter activity in transfection assays (17). KLF2 null mice die before E14.5, from a defect in the formation of the endothelium but also have reduced expression of embryonic ε-globin although expression of adult globin genes is normal (18).

KLF13 (KLF13 /BTEB3/FKLF2/RFLAT) is another xKLF protein expressed in the haematopoietic system (19,20). Binding of KLF13 activates the promoters of a number of erythroid genes including γ-globin, GATA-1, porphobilinogen deaminase and ferrochelatase *in vitro* (21). KLF13 is highly expressed in human peripheral blood lymphocytes and binds to and activates the RANTES promoter in late activated T cells (20,22). We showed that murine KLF13 was widely expressed during embryogenesis with high levels of expression in the developing heart, thymus and liver (19).

We have generated mice with a targeted deletion of exon one of the *Klf13* allele and found that these mice have enlarged hearts and an increased susceptibility to the formation of cardiac vacuolar lesions (Keramatipour et al. submitted). To determine the role of *Klf13* in the differentiation of erythroid cells we have compared erythropoiesis in $Klf13^{-/-}$ and $Klf13^{+/+}$ mice.

EXPERIMENTAL PROCEDURES

Mice

Klf13-/- mice generated in the CCB (129S6Sv/Ev) ES cell line were maintained on this genetic background. Genotyping of tail DNA was performed by PCR using primers CAG3F (GCCTCCGCTCGACGTCCCTAAGA) and CAG3R (GCGCGCTCTTCTCCGGCTG) to amplify the wild-type allele and INTF (CTGGGGATGCGGTGGGCTCTA) and INTR (GGGTGGCGAGACTCCAGCTC) to amplify the *Klf13* mutated allele. All mice were bred and maintained at the University of Cambridge Combined Animal Facility in accordance with the Animals (Scientific Procedures) Act 1986.

Blood Analysis

Blood was taken from the vena cava of $Klf13^{+/+}$ and $Klf13^{-/-}$ mice. Clotting was prevented by the addition of 0.5M tri-potassium-EDTA. Each sample was read in triplicate on an ABC Vet Automated Blood Counter (Woodley Equipment Company Ltd, Bolton, UK).

Flow Cytometry

Spleen and femur bones were dissected from 7-8 week old female $Klf13^{-/-}$ mice and $Klf13^{+/+}$. Body and spleen weights were recorded and splenocyte suspensions were made by mechanical dissociation through a 70μM strainer in the presence of cold PBS and 2% fetal calf serum (PBS/2%FCS). Bone marrow (BM) cells were extracted from femur bones using a 25G needle and resuspended in PBS/2%FCS.

Cells were stained using combinations of directly conjugated antibodies obtained from BD Pharmingen (San Diego, CA: anti-$CD4^{FITC}$, anti-$CD4^{PE}$, anti-$CD4^{Cychrome}$, anti-$CD8^{FITC}$, anti-$CD8^{PE}$, anti-$CD8^{Cychrome}$, anti-$CD3^{FITC}$, anti-$CD71^{FITC}$, anti-$Ter119^{PE}$, anti-$CD45^{PE}$, and anti-c-kit^{FITC}.

Cell suspensions were stained with the antibodies for 30 minutes on ice in 50 μL Dulbecco modified medium (Life Technologies, Gaithersburg, MD), supplemented with 5% fetal calf serum (FCS) and 0.01% sodium azide. Cells were washed in this medium between incubations and prior to analysis on the FACScan (fluorescence-activated cell scan; Becton

Dickinson, Franklin Lakes, NJ). Events were collected in list mode using CellQuest software (Becton Dickinson), and data were analyzed using CellQuest Pro software. Live cells were gated according to their FSC and SSC profiles. Data are representative of at least 3 experiments. Intracellular staining for cyclin B1 was performed on cells stained for surface markers as above following fixation and permeabilisation with the Cytofix/Cytoperm™ solutions (BD biosciences) according to the manufacturer's instructions.

Fluorescence Activated Cell Sorting (FACS) and Quantitative Reverse Transcription PCR (QRT-PCR)

Splenocyte suspensions were stained with antibodies against $CD19^{PE}$, (BD Pharmingen, San Diego, CA), $Ter119^{PE}$, and $CD71^{FITC}$ (eBioscience, San Diego, CA) before being sorted on a DakoCytomation MoFlo sorter. Only cells falling within the forward scatter/side scatter (FSC/SSC) live gate were sorted.

For purification using magnetic beads, splenocytes were incubated on ice with biotin labelled anti Ter119 at $1\mu g/10^6$ cells for 30 min before 50µl of streptavidin magnetic beads were added. After a further 10 min on ice the samples were placed against a magnet until the beads were against the side of the tube. Samples were washed by resuspension in PBS +2% FCS 3 times before being resuspended in 300µl of RLT buffer (Qiagen) for RNA purification.

Total RNA from sorted cells was extracted using RNAeasy (Qiagen, Valencia, CA). Reverse transcription and quantitative real-time PCR were performed as described previously (23). Primer sequences are available on request. *Klf13* transcript levels for each sample were normalised to rRNA levels which were amplified using TaqMan Universal PCR Master Mix (Applied Biosystems, Warrington, UK).

BFU-E and CFU-E colony forming assays.

BFU-E and CFU-E cultures were performed using the methocult system (StemCell Technologies) according to manufacturer's instructions. In brief, BM and spleen cells were plated at a density of 2 x 10(5) cells per ml 1% methylcellulose medium containing 15% FBS, 1% BSA, 10ug/ml insulin, 200ug/ml transferrin and 3U/ml EPO. Cultures were incubated at 37°C in 5% CO_2. CFU-E were enumerated after 2 days in culture and BFU-E after 3-4 days in culture. All cultures were done in duplicate and each experiment repeated eight times.

Statistical Analysis

Statistical analyses for differences between $Klf13^{+/+}$ and $Klf13^{-/-}$ mice were performed using the two tailed Student's *t* test assuming unequal variance. Data are presented as mean ± SD with n values given in the corresponding figure legends.

RESULTS

Generation of the Targeting Construct

A genomic clone containing the mouse *Klf13* gene (PAC F69-B12) was obtained by screening the mouse genome filter set RCP121 with the full length (1200 bp) *Klf13* coding sequence (Genbank accession No. AJ245644). *In silico* comparison of the *Klf13* coding sequence with the genomic sequence (ENSMUSG00000052040) together with experimental verification by Southern analysis and PCR showed that the *Klf13* gene consisted of two exons. Exon 1 codes for the transactivation domain and the first zinc finger of the protein and exon 2 codes for the other two zinc fingers. To identify the start of the first exon, the 5' end of the known coding sequence together with 200bp of presumed upstream sequence identified from the mouse htgs database was compared with the EST database using the BLAST algorithm. The majority of the EST sequences containing the 5' part of the *Klf13* coding sequence stopped at one of two positions separated by 30 nucleotides indicating the presence of two transcriptional start sites (Fig. 1A). The sequence upstream of the start sites did not contain a TATA box indicating that *Klf13* has a TATA-less promoter. To generate a vector to delete the first exon of *Klf13* a 1.5kb fragment (mouse chromosome 7, nucleotides 59688488 to 59689967) of the promoter region and 4.9 kb of the intron (chromosome 7, nucleotides 59682698 to 59687527) were amplified by PCR and cloned into the vector pKO-DTA along with a neomycin resistance cassette. All the fragments and the final targeting vector were sequenced to confirm the PCR fidelity and

to result in a null allele. The resulting vector pDPN is shown in Fig. 1B.

To generate recombinant ES cells with a targeted mutation in *Klf13*, pDPN was linearised in the vector backbone with *Pvu*II and electroporated into ES cells. Cells were selected in G418 and resistant clones were picked and expanded. DNA was extracted from 45 clones and amplified by PCR using primer PF and PR to identify clones with the appropriate 5' insertion of the DNA. This process identified 14 clones and DNA from these clones was digested with *Eco*RI and analysed by Southern blot. Probing the blot with a DNA probe to the 5kb intron gave a band >13kb for the wild-type locus and an 11kb band for the targeted locus (Fig. 1C). Twelve out of 45 clones contained the targeted locus giving an overall targeting frequency of 27% of the clones picked. The targeted ES cells were injected into C57Bl/6 blastocyts to generate transgenic mice.

***Klf13* null mice**

Genotyping of the offspring of the mice was performed by PCR for both the wild type and mutant alleles as shown in Fig 1D. This analysis showed that whilst null mice were detected after weaning, the numbers were less than that predicted by Mendelian inheritance (Table 1). To determine whether the lethality arose from an early embryonic loss, embryos from timed matings of $Klf13^{+/-}$ females with $Klf13^{-/-}$ males were examined and genotyped at E10.5 and E13.5. At neither of these time points was there any detectable deviation from Mendelian ratios (n=31 embryos at E=10.5 with 14 $Klf13^{-/-}$ and 17 $Klf13^{+/-}$ embryos; n= 59 embryos at E13.5 with 30 $Klf13^{+/-}$ embryos and 29 $Klf13^{-/-}$ embryos). The cause and time of onset of the lethality has yet to be determined. To confirm that the $Klf13^{-/-}$ mice did not express KLF13 mRNA, RNA from the heart (a tissue which expresses high levels of KLF13) was reverse transcribed and amplified by PCR. KLF13 mRNA was not detectable by this method in $Klf13^{-/-}$ mice (Fig 1E). Quantification of mRNA from the heterozygous animals suggested that these mice expressed approximately half of the mRNA levels expressed in wild-type mice (Fig 1F). It is therefore likely that KLF13 does not

Altered blood cell composition in $Klf13^{-/-}$ mice

To determine the effect of loss of KLF13 on the haematopoietic system, blood samples were taken and complete blood counts determined. Whilst the haematocrit of $Klf13^{-/-}$ mice was the same as wild type mice the numbers of red cells were reduced by 10% and their size (MCV) was increased (see Table 2). Consequently the blood of the $Klf13^{-/-}$ mice was populated with fewer but larger red blood cells. Despite the altered erythrocyte profile, total haemoglobin levels in the $Klf13^{-/-}$ mice were unaltered. $Klf13^{-/-}$ mice also had reduced numbers of lymphocytes (to 70% of wild type) and a trend towards reduced numbers of granulocytes (to 76% of wild-type) and monocytes (to 77% of wild-type) suggesting that the loss of KLF13 affects the pathways involved in the differentiation or survival of the major blood cell types (Table 2). To investigate the cause of the change in erythrocytes in the blood we analysed the cellular composition of the spleen.

Increased spleen size in $Klf13^{-/-}$ mice

Spleens removed from 7 week old $Klf13^{-/-}$ mice were approximately 1.5 times the weight of those removed from age and sex matched $Klf13^{+/+}$ mice (117±27 mg $Klf13^{-/-}$ and 73±11mg $Klf13^{+/+}$). Similar results were obtained with the spleen weights normalised to body weight (5.5±1.2 mg/g body weight $Klf13^{-/-}$ and 3.73±0.6 mg/g body weight $Klf13^{+/+}$, Fig, 2A). Furthermore, there was a proportionate increase in the number of cells isolated from the spleens of $Klf13^{-/-}$ mice compared to their $Klf13^{+/+}$ counterparts (Fig 2B) indicating that the increase in spleen size is due to an increase in cell number rather than fibrosis.

Flow cytometry using anti-CD3ε and anti-CD19 showed a reduction in the proportions of T and B cells in the spleens of $Klf13^{-/-}$ mice (Fig 2C) which when adjusted for spleen cell number showed no difference in absolute lymphocyte number between $Klf13^{-/-}$ and $Klf1^{+/+}$ mice. Consequently the proportion of cells that did not stain for CD3ε or CD19 increased from 10% in the wild type mice to 33% in the $Klf13^{-/-}$ mice. These data indicate that the increased

splenomegaly. Staining the cells for CD45 identified three cell populations CD45^{-} (Fig 2D), CD45^{med} (Fig 2D upper left) and CD45^{hi} (Fig 2D upper right). .The number of CD45^{hi} cells did not change (*Klf13*$^{+/+}$; 1.05 ± 0.06 x 10^8 cells/spleen and *Klf13*$^{-/-}$; 0.98 ± 0.2 x 10^8 cells/spleen) but there was a marked 7-fold increase (*Klf13*$^{+/+}$; 5.8 ± 2.3 x 10^6 cells/spleen and *Klf13*$^{-/-}$; 43.7 ±11.0x 10^6 cells/spleen) in the number of CD45^{med} cells and a 3-fold increase in the number of CD45^{-} cells in the spleens of *Klf13*$^{-/-}$ mice (*Klf13*$^{+/+}$; 12.6 ± 0.17 x 10^6 cells/spleen and *Klf13*$^{-/-}$; 41.8 ± 0.74 x 10^6 cells/spleen., Fig. 2E). As CD45 is highly expressed on the majority of lymphoid and myeloid cells it was unlikely that the increased spleen mass in *Klf13*$^{-/-}$ mice was attributable to cells of these lineages. However, during erythroid cell development, Expression of CD45 decreases as erythroblasts mature into erythrocytes suggesting that the increase in spleen size in *Klf13*$^{-/-}$ mice could be due to alterations in the erythroid lineage.

Abnormal erythroblast maturation in *Klf13*$^{-/-}$ mice

To determine whether the increase in cell number was due to an expansion of cells of the erythroblast lineage, splenocytes from *Klf13*$^{-/-}$ and *Klf13*$^{+/+}$ mice were stained for Ter119 and CD71. The expression of these markers distinguishes at least four populations of erythroid cells which are, from least to most differentiated, Ter119^{med}CD71^{hi}, Ter119^{hi}CD71^{hi}, Ter119^{hi}CD71^{med} and Ter119^{hi}CD71^{low} Fig 3A (3). These populations are represented in Figure 3B as I, II, III and IV respectively and can be further characterised by their size with an overall decrease in cell size from type I to Type IV. flow cytometric analysis (Fig. 3A) showed a seven fold expansion of Ter119^{med}CD71^{hi} from 2.2 ± 1.0 x 10^5 cells/spleen in the *Klf13*$^{+/+}$ mice to 15.6 ± 8.9 x 10^5 cells/spleen in the *Klf13*$^{-/-}$ mice, and Ter119^{hi}CD71^{hi} from 3.4 ± 2.3 x 10^6 cells/spleen in the *Klf13*$^{+/+}$ mice to 15.6 x 10^6 cells/spleen in the *Klf13*$^{-/-}$ mice and a three fold expansion of Ter119^{hi}CD71^{med} from 9.3 x 10^6 cells/spleen in the *Klf13*$^{+/+}$ mice to 21.9 x 10^6 cells/spleen in the *Klf13*$^{-/-}$ mice (Fig. 3B). However, despite this increase in erythroid precursors, numbers of late erythroblasts (Ter119^{hi}CD71^{low}, chromatophilic erythrobalsts to reticulocytes) remained unaltered.

The alterations in erythropoiesis may have resulted from indirect effects rather than loss of KLF13 in the erythroblasts. We therefore determined whether *Klf13* was expressed in erythroblasts. Quantifying *Klf13* mRNA in erythroblasts sorted by FACS from the spleens of *Klf13*$^{+/+}$ mice showed that *Klf13* expression increased between Ter119^{+}CD71^{+} erythroblasts and Ter119^{+}CD71^{-} erythroblasts (2.5-fold, Fig. 3C). These levels of *Klf13* mRNA in Ter119^{+}CD71^{-} erythroblasts are similar to those in splenic CD4^{+} and CD8^{+} T cells CD19^{+}, and 10-fold higher than splenic B cells (Outram, *et al.* submitted). Therefore, *Klf13* expression increases as erythroid precursors mature suggesting a direct involvement of KLF13 in erythroblast differentiation.

Erythropoiesis in the BM

Whilst some erythropoiesis occurs in the spleen under normal conditions, most splenic erythropoiesis occurs as a response to haematologic stress (5). The process of normal erythropoiesis occurs mostly in the BM. Therefore to determine whether the same defects occurred in erythropoiesis in the BM we determined the proportion of type I to type IV cells in the BM. This analysis showed an increase in type II erythroblasts ($p<0.03$) in the BM and a trend to an increase in the number of type I cells but this did not reach significance ($p=0.06$). There was no effect on the other erythroblast populations (Fig. 3D).

To analyse the ability of progenitors from *Klf13*$^{-/-}$mice to differentiate along the erythropoietic lineage we determined the number of BFU-Es and CFU-Es in the spleen. Consistent with the increase in Ter119^{med}CD71^{hi} cells both BFU-Es and CFU-Es were increased in the spleen (Figs 3E and 3F). In the BM there was no change in the number of CFU-E or BFU-E. Together with the CD71/Ter119 staining these data suggest that loss of KLF13 does not inhibit the commitment of cells to the erythrocyte lineage.

Expression of transcription factors involved in erythropoiesis

To determine whether the expression of other transcription factors known to be

erythrocytes was altered by the lack of *Klf13*, we determined the expression of *GATA-1*, *KLF1* and *KLF3* by Q-RTPCR in Ter119^{+} cells isolated by magnetic bead separation from the spleens of *Klf13*$^{-/-}$ and *Klf13*$^{+/+}$ mice. The mRNA for all of these transcription factors increased at least 3-fold in the erythroblasts of *Klf13*$^{-/-}$ mice (Fig. 4A). It is possible that the increase in the mRNA for these transcription factors was due to differences in the proportion of immature Ter119^{+} cells in the samples from the different mice. We therefore compared the expression of the same factors in the FACS sorted Ter119^{+}CD71^{-} and Ter119^{+}CD71^{+} cells from *Klf13*$^{+/+}$ mice. The mRNAs for both *GATA-1* and KLF1 were 4-6 fold higher in the Ter119^{+}CD71^{+} cells (Fig. 4B) making it likely that the increase in these mRNAs results from an increase in the number of less mature cells in the *Klf13*$^{-/-}$ mice. However, the expression of *Klf3* was lower in Ter119^{+}CD71^{+} cells compared to Ter119^{+}CD71^{-} indicating that loss of KLF13 had resulted in an increase in *Klf3* expression (Fig. 4A).

Erythroid cell proliferation in KLF13$^{-/-}$ mice

To determine whether the loss of *Klf13* altered the proliferation of erythroblasts cyclin B expression was measured in Ter119^{med} and Ter119^{hi} cells. Cyclin B expression was increased in Ter119^{med} cells but not in Ter119^{hi} cells of the *Klf13*$^{-/-}$ mice. These data indicate that the cell proliferation increased in type I cells but not in more mature erythroblasts (Fig. 5A).

Altered expression of apoptosis associated genes in KLF13$^{-/-}$ mice

The final stages of erythroid differentiation requires the expression of genes associated with apoptosis (2). Therefore, we determined the expression of the major determinants of apoptosis in Ter119^{+ve} cells by Q-RT-PCR. This analysis showed that there was no change in the expression of Bad or Bcl-2 and a trend towards an increase in the expression of Bax but this did not reach significance (Fig. 5B). However there was a marked (4.5 fold) increase in the expression of Bcl-xL in the splenocytes from *Klf13*$^{-/-}$ mice compared to their wild-type counterparts (Fig. 5B). To determine whether this increase in Bcl-xL was due to the increase in the proportion of CD71 positive cells in the Ter119^{+} population Bcl-xL, Bad and Bax and Bcl2 were measured in FACS sorted populations of CD71^{+}:Ter119^{+} and CD71^{-}:Ter119^{+} splenocytes from wild-type mice. This analysis showed that Bcl-xL expression was higher in the CD71^{+}:Ter119^{-} cells than in the CD71^{+}:Ter119^{+} cells consequently much of the increased amount of Bcl-xL observed in the KLF13$^{-/-}$ mice is likely to arise from the increase in proportion of immature cells in the spleens of these mice (Fig 5C). Consistent with these observations we did not observe a significant reduction in apoptosis in Ter119^{+} cells by annexin staining. During the preparation of this paper Zhou et al (24) published their analysis of a similar line of KLF13$^{-/-}$ mice. This analysis showed a marked reduction in apoptosis and increased expression of Bcl-xL in thymocytes. Thus it appears that Bcl-xL is a major target of KLF13 in thymocytes but not in erythrocytes.

DISCUSSION

Previous studies have implicated *Klf13* in the differentiation of erythrocytes *in vitro*(17,22). Our data demonstrate a role for *Klf13* in these cells *in vivo* by showing that there is an increase in the number of immature erythrocytes in the spleens of mice that lack expression of *Klf13*. Indeed the reduced levels of other cell types in the circulation of the *Klf13*$^{-/-}$ mice suggest that *Klf13* is required for the differentiation and/or proliferation of other haematopoietic cell lineages.

Our data indicate that the cells were able to commit to the erythrocyte lineage as there was no change in the number of BFU-Es or CFU-Es in the bone marrow. However the cells accumulate in the proerythroblast stage of development and have increased expression of KLF3. Mice that lack KLF3 have also been shown to have splenomegaly although the mechanism behind this phenotype is unexplored raising the possibility that both KLF13 and KLF3 act at the same point but that the increase in KLF3 is insufficient to overcome the loss of KLF13. An alternative explanation of these data is that KLF13 is an inhibitor of *Klf3* expression in erythroblasts.

Erythropoiesis is disrupted in several other lines of mice with targeted mutations to transcription factors. For example, both GATA-1 and KLF1 are required for erythropoiesis to occur mice (8,16). Mice with low levels of expression of GATA-1 survive but become increasingly anaemic with age (25) and show stress erythropoiesis as a compensation for defective primary erythropoiesis. This phenotype is similar to that seen in *lyn*$^{-/-}$ mice which have reduced expression of *GATA*-1 and KLF1 (26). The splenomegaly observed in our mice is also consistent with a stress erythropoietic response. However, in our mice we found little change in the expression of both *Klf1* and *GATA-1* in Ter119^{+} cells in contrast to the data from *lyn*$^{-/-}$ mice. This difference suggests that *Klf13* regulates a different stage of erythropoiesis to that regulated by KLF1 and GATA-1. Furthermore, it suggests that although KLF13 is known to bind to and activate the GATA-1 promoter it is not a major regulator of GATA-1 expression. However, it is also possible that KLF13 interacts with and/or cooperates with GATA-1 to drive a subset of GATA-1 functions in erythropoiesis. Such an interaction has recently been shown between GATA-4 and KLF13 in *Xenopus* and results in a failure of cardiac development and a reduction in the expression of B-type naturietic peptide in this model (27). The extent of any requirement for KLF13 in the function of GATA-1 is also dependent on the ability of other KLF proteins to compensate for the loss of KLF13 in some but not all activities of GATA-1.

Apoptosis of erythrocytes occurs in the spleen as a feedback mechanism to regulate the number of erythrocytes and splenomegaly has been shown in mice with aberrant apoptosis(28,29). It was therefore possible that loss of *Klf13* resulted in a reduction in apoptosis and consistent with this suggestion during the preparation of this paper Zhou et al (24) published their analysis of *Klf13*$^{-/-}$ mice and showed that KLF13 was an inhibitor of the expression of the antiapoptotic factor Bcl-xL. However, in our mice there was no significant change in annexin staining in Ter119^{+} cells suggesting that there was no increase in apoptosis in these mice. Furthermore we found no detectable increase in Bcl-xL expression once the change in proportion of immature cells was accounted for. However, we did detect an increase in the expression of cyclin B in Ter119^{+} cells suggesting an increase in proliferation. Together these data suggest that increased proliferation rather than a reduction in apoptosis leads to the increase in spleen size.

In summary the data presented here identify a role for *Klf13* in the maturation of erythrocytes. Loss of *Klf13* results in an increase in the expression of *Klf3* and cyclin B but other *Klf13* target genes in erythroblasts remain to be identified.

Acknowledgements

Funding

This work was supported by the British Heart Foundation grant No PG/02/135/14620 to P.K and J.M. S.O was supported by the BBSRC and AH-T was supported by the Wellcome Trust. CG was supported by the MRC**,** WHC was supported by the Ford Physiology endowment fund.

The authors have no competing financial interests.

References

1. Perry, C., and Soreq, H. (2002) *Eur J Biochem* **269**, 3607-3618
2. Koury, M. J., Sawyer, S. T., and Brandt, S. J. (2002) *Curr Opin Hematol* **9**, 93-100
3. Zhang, J., Socolovsky, M., Gross, A. W., and Lodish, H. F. (2003) *Blood* **102**, 3938-3946
4. Hara, H., and Ogawa, M. (1976) *Am J Hematol* **1**, 453-458
5. Kam, H. Y., Ou, L. C., Thron, C. D., Smith, R. P., and Leiter, J. C. (1999) *J Appl Physiol* **87**, 1901-1908
6. Moritz, K. M., Lim, G. B., and Wintour, E. M. (1997) *Am J Physiol* **273**, R1829-1844
7. Wall, L., deBoer, E., and Grosveld, F. (1988) *Genes Dev* **2**, 1089-1100
8. Fujiwara, Y., Browne, C. P., Cunniff, K., Goff, S. C., and Orkin, S. H. (1996) *Proc Natl Acad Sci U S A* **93**, 12355-12358
9. Kaczynski, J., Cook, T., and Urrutia, R. (2003) *Genome Biol* **4**, 206
10. Perkins, A. (1999) *Int J Biochem Cell Biol* **31**, 1175-1192

11. Feinberg, M. W., Cao, Z., Wara, A. K., Lebedeva, M. A., Senbanerjee, S., and Jain, M. K. (2005) *J Biol Chem* **280**, 38247-38258
12. Matsumura, T., Suzuki, T., Aizawa, K., Munemasa, Y., Muto, S., Horikoshi, M., and Nagai, R. (2005) *J Biol Chem* **280**, 12123-12129
13. Song, C. Z., Keller, K., Chen, Y., and Stamatoyannopoulos, G. (2003) *J Mol Biol* **329**, 207-215
14. Ellenrieder, V., Zhang, J. S., Kaczynski, J., and Urrutia, R. (2002) *Embo J* **21**, 2451-2460
15. Miller, I. J., and Bieker, J. J. (1993) *Mol Cell Biol* **13**, 2776-2786
16. Perkins, A. C., Sharpe, A. H., and Orkin, S. H. (1995) *Nature* **375**, 318-322
17. Zhang, P., Basu, P., Redmond, L. C., Morris, P. E., Rupon, J. W., Ginder, G. D., and Lloyd, J. A. (2005) *Blood Cells Mol Dis* **35**, 227-235
18. Wani, M. A., Means, R. T., Jr., and Lingrel, J. B. (1998) *Transgenic Res* **7**, 229-238
19. Martin, K. M., Metcalfe, J. C., and Kemp, P. R. (2001) *Mech Dev* **103**, 149-151.
20. Song, A., Chen, Y. F., Thamatrakoln, K., Storm, T. A., and Krensky, A. M. (1999) *Immunity* **10**, 93-103.
21. Asano, H., Li, X. S., and Stamatoyannopoulos, G. (2000) *Blood* **95**, 3578-3584
22. Nikolcheva, T., Pyronnet, S., Chou, S. Y., Sonenberg, N., Song, A., Clayberger, C., and Krensky, A. M. (2002) *J Clin Invest* **110**, 119-126.
23. Ellis, P. D., Smith, C. W., and Kemp, P. (2004) *J Biol Chem* **279**, 36660-36669
24. Zhou, M., McPherson, L., Feng, D., Song, A., Dong, C., Lyu, S. C., Zhou, L., Shi, X., Ahn, Y. T., Wang, D., Clayberger, C., and Krensky, A. M. (2007) *J Immunol* **178**, 5496-5504
25. Takahashi, S., Komeno, T., Suwabe, N., Yoh, K., Nakajima, O., Nishimura, S., Kuroha, T., Nagasawa, T., and Yamamoto, M. (1998) *Blood* **92**, 434-442
26. Ingley, E., McCarthy, D. J., Pore, J. R., Sarna, M. K., Adenan, A. S., Wright, M. J., Erber, W., Tilbrook, P. A., and Klinken, S. P. (2005) *Oncogene* **24**, 336-343
27. Lavallee, G., Andelfinger, G., Nadeau, M., Lefebvre, C., Nemer, G., Horb, M. E., and Nemer, M. (2006) *Embo J* **25**, 5201-5213
28. Diwan, A., Koesters, A. G., Odley, A. M., Pushkaran, S., Baines, C. P., Spike, B. T., Daria, D., Jegga, A. G., Geiger, H., Aronow, B. J., Molkentin, J. D., Macleod, K. F., Kalfa, T. A., and Dorn, G. W., 2nd. (2007) *Proc Natl Acad Sci U S A* **104**, 6794-6799
29. Rhodes, M. M., Kopsombut, P., Bondurant, M. C., Price, J. O., and Koury, M. J. (2005) *Blood* **106**, 1857-1863

Figure legends

Figure 1. Targeting the *Klf13* locus

A. The 5' region of the *Klf13* mRNA. Start sites identified by BLAST comparison with the EST database are indicated by (_) and the translation start site is underlined. **B**. The wild-type *Klf13* locus, linearised targeting construct and targeted allele are shown. *Klf13* exons are shown as filled black rectangles. Boxes marked Neo and DT-A show the positions of the neomycin and Diphtheria toxin A selection cassettes respectively. Arrows mark the positions of primers used for genotyping (1; B3F, 2; B3R, 3; MutF, 4; MutR). The positions of EcoRI sites are marked by E and the probe used for Southern hybridisation is marked by a thick line. **C.** Southern analysis of ES cell clones. DNA extracted from ES cells was digested with EcoRI. Southern blots of the DNA were probed with a 4kb fragment of the intron. **D**. PCR genotyping of wild-type, heterozygous and homozygous null mice. DNA from ear clips was amplified using primers B3F, B3R, MutF and MutR and the products analysed on a 2% agarose gel. The bands sizes are 185bp (wild type) and 226bp (mutant). **E**. RT-PCR for *Klf13* mRNA in the hearts of $Klf13^{+/+}$, $Klf13^{+/-}$ and $Klf13^{-/-}$ mice. *Klf13* mRNA produces a 185bp product. No products were observed in the absence of reverse transcription indicating that the samples were not contaminated with genomic DNA. M. Marker lane (Hyperladder I). **F**. Relative expression of KLF13 determined by quantitative real-time PCR of cDNA from the right ventricle (n=5 samples for each genotype). Messenger RNAs were quantified by calculating C_t and normalised to the C_t value for rRNA as described previously[14]

Figure 2. Deletion of *Klf13* results in increased spleen size

Spleens were taken from 7 week old female $Klf13^{-/-}$ mice and their wild-type counterparts. The spleens were weighed and compared to the body weight of the mouse (n=26 of each genotype) (**A**). Splenocyte suspensions were prepared as described in Materials and Methods and the cells counted on a haemocytometer (n=7 of each genotype) (**B**). Cell suspensions were stained with anti-CD19 and anti-CD3 and analysed by flow cytometry. There was a large increase in the percentage (3 fold, n = 12 mice) of unstained cells. Cell percentages from a representative experiment are shown (**C**). Cells were stained for CD45; $CD45^-$ (bottom left hand area), $CD45^{med}$ (box R2) and $CD45^{hi}$ (box R3) (**D**). The cells in these areas were quantified and normalised to the average for wild-type mice (E) (n = 6 mice for each line). All data are mean ± SD, * $p<0.02$, ** $p<0.005$, *** $p<0.0001$ wt vs $Klf13^{-/-}$)..

Figure 3. Increased erythropoiesis in in $Klf13^{-/-}$ mice

A. Ter119 and CD71 staining of splenocytes from $Klf13^{-/-}$ and wild-type mice identified four erythroblast populations (I to IV; values given are mean percentages corrected for spleen size). The overlay plots shows the CD71 fluorescence profile of populations II and III from a wild-type and $klf13^{-/-}$ mouse. The four populations identified in (A) populations were quantified (**B**) and normalised to the average number in wild type mice (data are mean ± SD, n = 6 mice for each line). Clear bars represent wild-type and b1ack bars represent $Klf13^{-/-}$ mice. **C**. Splenocytes from wild-type mice were stained with antibodies to ter119 and CD71 and sorted by FACS. A minimum of 10^5 cells were collected for each population and the RNA extracted. RNA was reverse transcribed and amplified in real-time PCR reactions using primers for *Klf13*. *Klf13* mRNA was normalised to rRNA. **D**. Femoral bone marrow cells were stained with Ter119 and CD71 and separated by FACS. The four erythroblast populations were quantified and normalised to the average number in wild-type mice (n = 6 mice of each genotype). Splenocytes and bone marrow cells from wild type and $Klf13^{-/-}$ mice were cultured in methylcellulose as described in Materials and Methods. Numbers of CFU-E colonies (**E**) and BFU-E colonies (**F**) on each plate were normalised to the average number of colonies on the plates from wild-type mice (n=8 for each line). All data are presented as mean ± SD, * $p<0.03$, ** $p<0.01$ wt vs $Klf13^{-/-}$)

Fig 4. Effect of loss of Klf13 on the expression of *Gata-1*, *Klf1*, and *Klf3*

RNA was extracted from (**A**) Ter119 positive splenocytes isolated on magnetic beads or (**B**) Ter119 and CD71 stained, FACS sorted splenocytes. *Gata-1*, *Klf1*, and *Klf3* mRNAs were quantified by quantitative real-time PCR normalised to *Gapdh* (n = 5 mice for each line, mRNA samples were

prepared and analysed from each mouse independently). Data are presented as mean ± SD, * $p<0.03$ wt vs *Klf13*$^{-/-}$.

Figure 5. Cell proliferation and apoptosis in *Klf13*$^{-/-}$ mice

Splenocytes were stained for Ter119 and cyclin B (**A**). Spleens from *Klf13*$^{-/-}$ mice had increased numbers of Ter119^{med} cells expressing cyclin B1 compared to those of wild-type mice (n=3 mice of each genotype). RNA was extracted from (**B**) Ter119 positive splenocytes isolated on magnetic beads or (**C**) Ter119 and CD71 stained, FACS sorted splenocytes. *Bcl-XL*, *Bad, Bax*, and *Bcl2* mRNAs were quantified by quantitative real-time PCR normalised to *Gapdh* (n = 5 mice for each line, mRNA samples were prepared and analysed from each mouse independently). Data are presented as mean ± SD, * $p<0.05$, ** $p<0.01$, wt vs *Klf13*$^{-/-}$).

Table 1. Genotype ratios of mice born to KLF13$^{+/-}$ parents

Offspring number	+/+	+/-	-/-
actual	131	285	98
predicted	129	258	129
	Chi squared =10.3 p<0.01		

Table 2. Blood cell counts

	Klf13$^{+/+}$			*Klf13*$^{-/-}$		
	MEAN (n=5)	STDEV	Reference range (mean ± 2SD)	MEAN (n=4)	STDEV	t-test p value
WBC	9.36	0.78	10.9-7.8	6.75	0.89	0.003
RBC	10.54	0.52	11.5-9.5	9.54	0.55	0.03
HGB	16.7	0.5	17.6-15.7	16.0	0.84	NS
HCT	51	1.50	53.9-47.9	49.0	2.44	NS
MCV	48.3	1.55	51.4-45.2	51.5	0.43	0.008
MCH	15.9	0.46	16.7-14.9	16.8	0.19	0.006
MCHC	32.7	0.24	33.1-32.25	32.7	0.08	NS
PLTS	458	50	557-358	437	113.42	NS
MPV	5.03	0.09	5.21-4.85	4.98	0.13	NS
RDW	13.71	0.42	14.5-12.9	14.36	0.11	0.024
LYMP	6.50	0.69	7.88-5.12	4.56	0.51	0.002
MONO	1.33	0.06	1.45-1.21	1.01	0.21	0.054
GRAN	1.53	0.22	1.97-1.09	1.18	0.28	0.08

Legend

WBC; white blood cell count (x10^3/mL), RBC red blood cell count (x10^6/ul), HGB; haemoglobin concentration (g/dL), HCT; haematocrit (%), MCV mean corpuscle volume (fL), MCH; mean corpuscle haemoglobin (pg), MCHC, mean corpuscle haemoglobin concentration (g/dL), PLTS; number of platelets (x 10^3/ul), MPV; mean platelet volume (fL), RDW; red cell distribution width, Lymp; lymphocyte number (x10^3/mL), Mono; Monocyte number (x10^3/mL), Gran; granulocyte number (x10^3/mL). The reference range has been calculated as 2 standard deviations from the mean of the wild-type population.

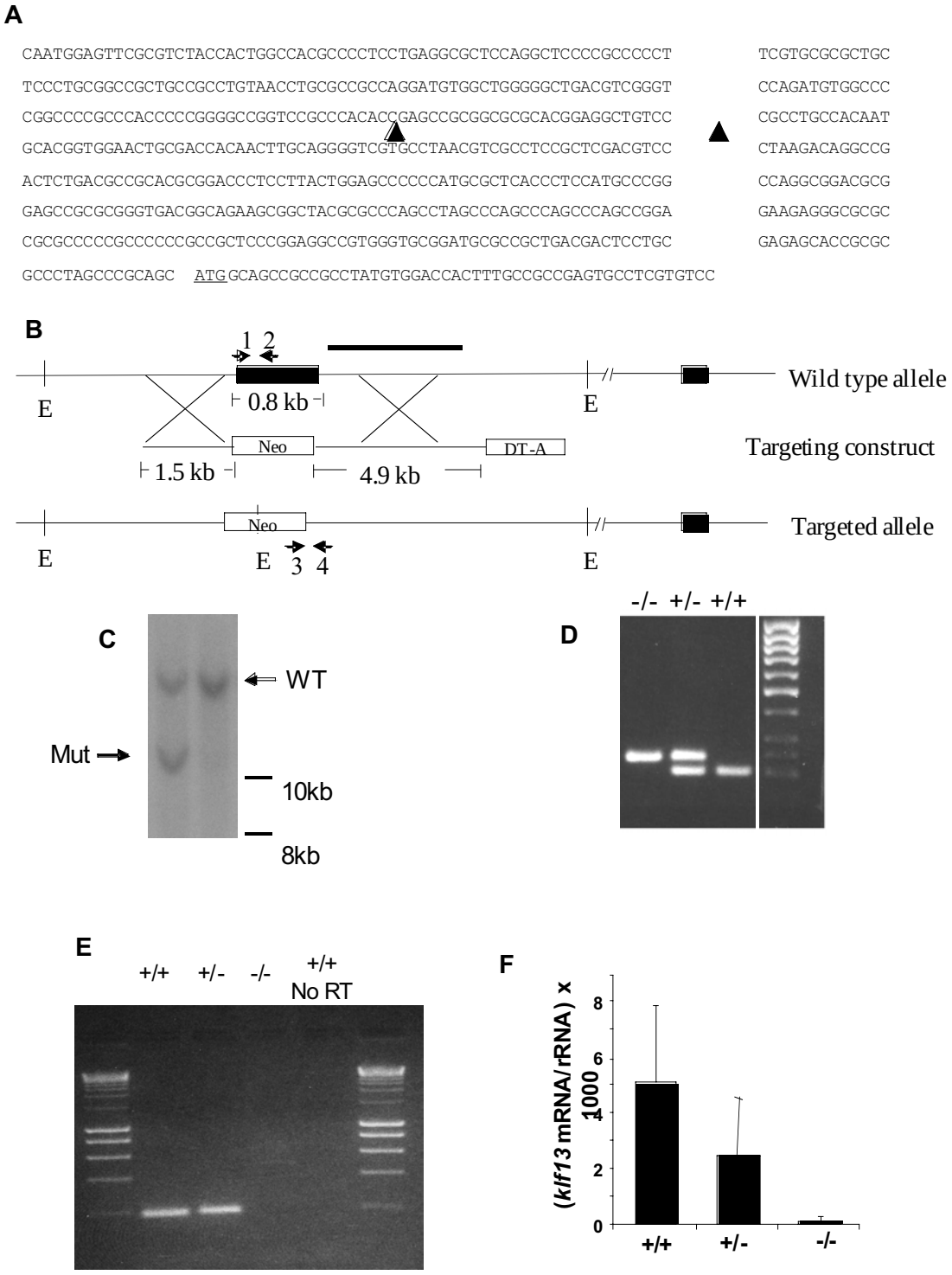

Gordon Outram et al Figure 1

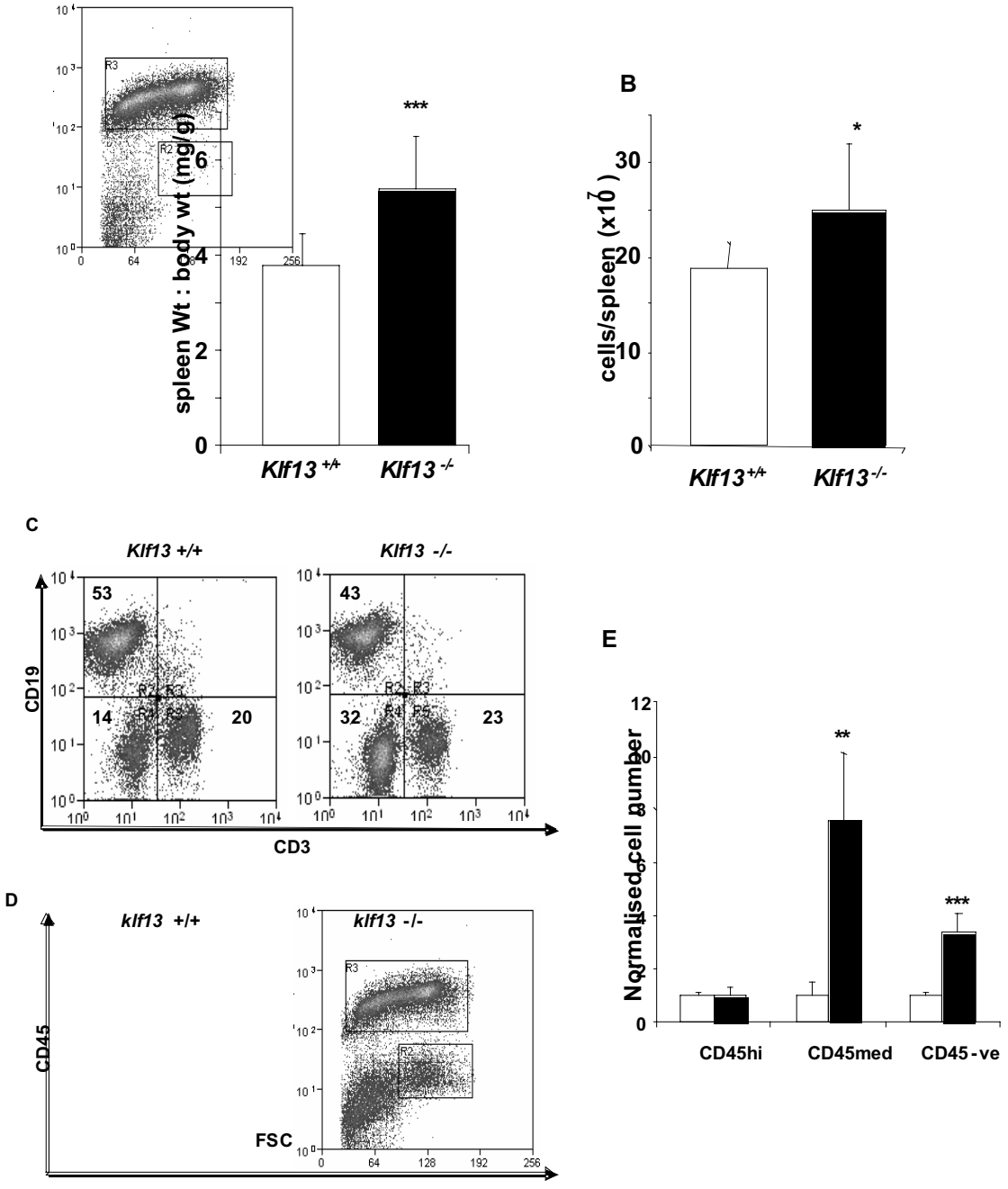

Gordon, Outram et al Fig. 2

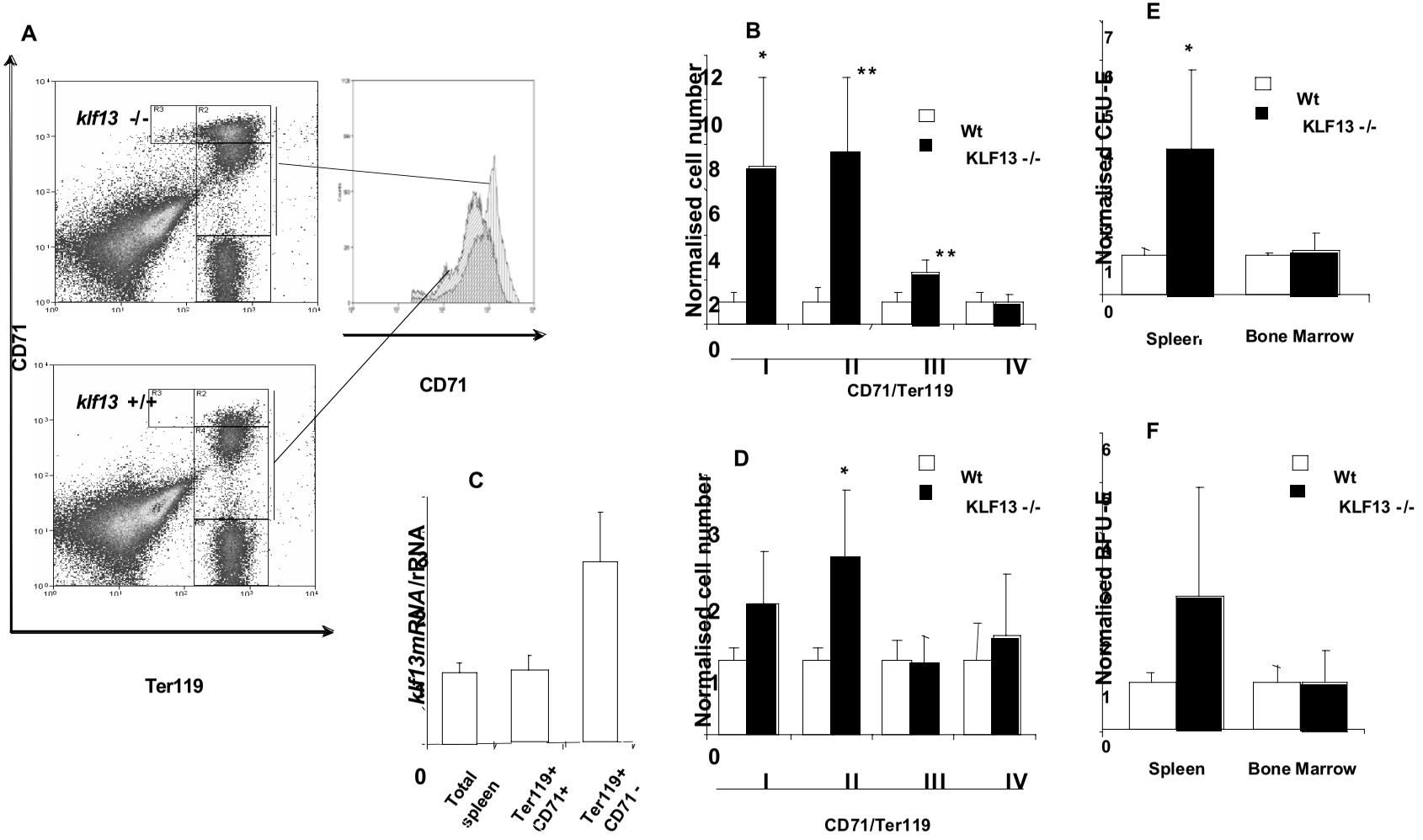

Gordon, Outram et al fig 3

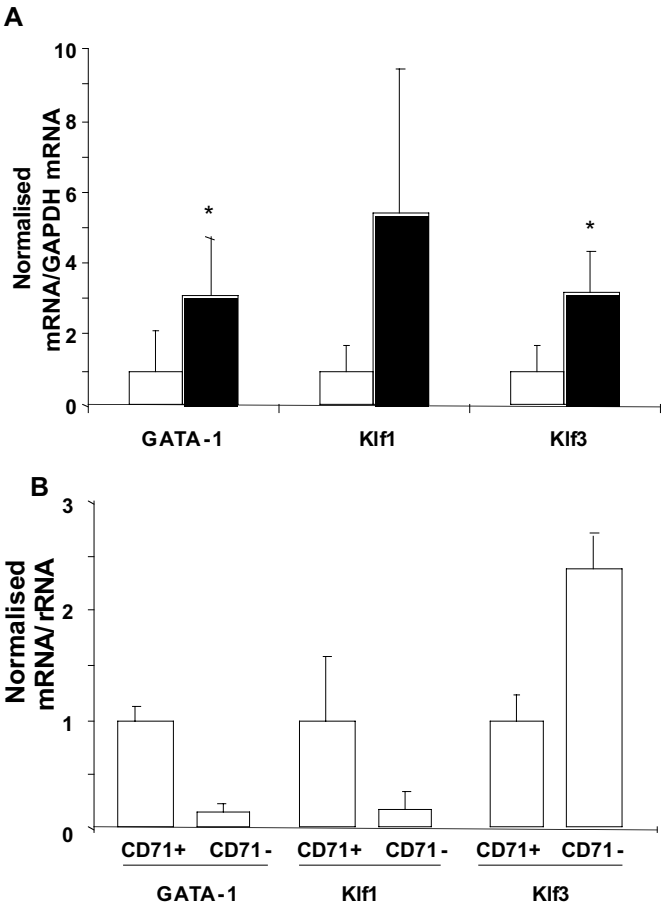

Gordon, Outram et al Fig. 4

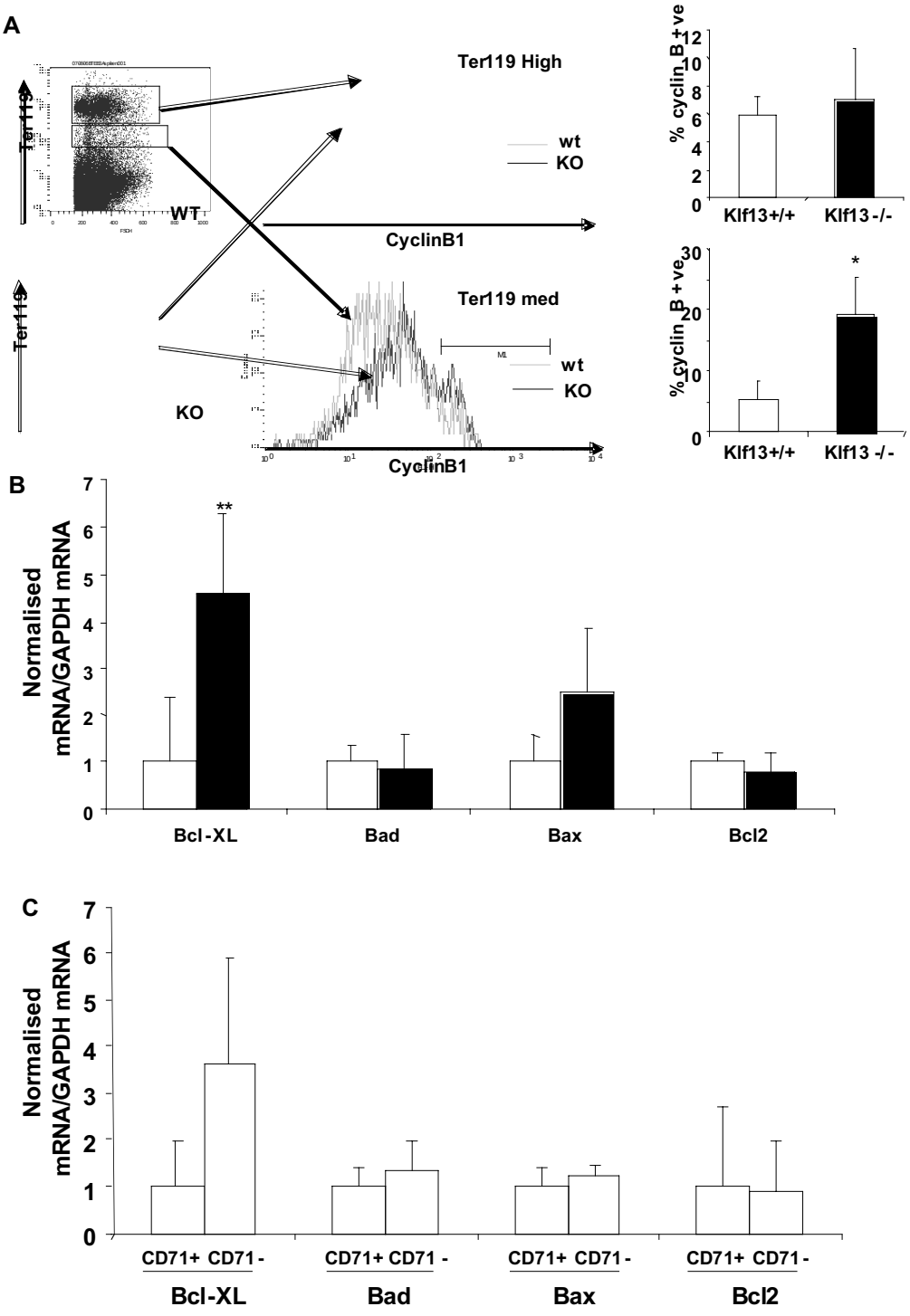

Gordon, Outram et al Fig. 5